RS
4,5

580

Influencing factors and countermeasures of aging and yellowing on windshield rubber in high-speed train

Received 1 August 2025
Revised 25 August 2025
Accepted 8 September 2025

Wei Du
Metals and Chemistry Research Institute, Fem Research Institute for Precious Metals and Metal Chemistry, Beijing, China

Abstract

Purpose – Regarding that Ultraviolet radiation, pollutant adsorption, and environmental changes may be the main reasons for the aging and yellowing on windshield rubber in high-speed trains, countermeasures are proposed to solve the aging and yellowing of windshield rubber and reduce the adverse effects caused by rubber yellowing.

Design/methodology/approach – Scanning electron microscopy (SEM) and energy dispersive spectroscopy (EDS) were used to test the yellowed windshield rubber. Aging tests, including UV aging, natural aging and salt spray aging, were conducted to analyze the effects of aging on the windshield rubber. Different cleaning agents were selected to soak the windshield rubber, and the quality, hardness, and surface appearance of the rubber samples were tested.

Findings – After UV aging, antioxidants migrated to the surface of the windshield rubber, but due to oxidation failure, they could not capture free radicals, leading to continued oxidation reactions within the material and resulting in yellowing of the rubber in a short period of time.

Originality/value – Cleaning agents have a minimal impact on windshield rubber, UV aging has the greatest impact and natural aging is a gradual and slow deterioration process. Through daily deep cleaning and maintenance with protective agents at regular intervals, the deterioration of windshield rubber yellowing in high-speed trains can be effectively suppressed.

Keywords High-speed train, Windshield rubber, Aging and yellowing, Countermeasures

Paper type Research article

1. Introduction

As the core carrier of modern rail transit, the efficient and safe operation of high-speed trains relies on the collaborative innovation and system integration of multiple key technologies. As a key functional component of the train, the windshield plays multiple roles in reducing aerodynamic resistance, optimizing noise control, and ensuring the sealing of the train end. There are three types of windshields between the two vehicles: compression type external windshield, airtight internal windshield, and snow proof windshield. The compression type external windshield plays a role in reducing the resistance of flowing air. The airtight internal windshield ensures the airtightness of the vehicle's interior, while the anti snow windshield is designed specifically for harsh weather conditions to prevent snow and dust from entering the car. The problem of aging and yellowing not only affects aesthetics, but may also lead to degradation of material properties, thereby reducing the overall image of the vehicle and passenger experience.

Windshield yellowing is primarily caused by the combined effects of environmental aging and material properties. Ultraviolet radiation triggers photo-oxidative degradation of

Railway Sciences
Vol. 4 No. 5, 2025
pp. 580-597
Emerald Publishing Limited
e-ISSN: 2755-0915
p-ISSN: 2755-0907
DOI 10.1108/RS-08-2025-0025

aromatic compounds in rubber or coatings, generating quinone chromophores (Yu, Sun, Ma, & Zhang, 2019; Liu, Qi, Wan, & Zheng, 2022; Zhang, Zeng, Song, & Wang, 2024; Wu, Wang, & Wang, 2017; Kim, Lee, & Yang, 2016; Celina, 2013; Yang & Jiang, 2011; Ge, 2010). Additionally, high-speed operation exposes the windshield to sand impact, contamination (such as industrial particles and exhaust oil films), and temperature-humidity cycles, further accelerating surface fading and yellow spot formation, as shown in Figure 1. Currently, some rubber windshields on existing high-speed trains have exhibited discoloration and yellowing, severely affecting the appearance and product quality of high-speed trains. Previous studies have mostly focused on the impact of a single factor (such as ultraviolet radiation or pollutants) on rubber aging, but there are few related studies on multi factor coupled aging testing. Through experiments, it has been confirmed that UV aging (photo oxidative degradation), natural aging, salt spray aging, and cleaning agents have a synergistic effect, revealing that multiple factors jointly trigger rapid yellowing of windshield rubber. (Xu, Song, Zheng, & Hu, 2007; Tang *et al.*, 2023; Kim, Kim, & Cho, 2025; Huang, Wang, Qiu, & Wu, 2016; Jiang, Zheng, Song, Li, & Wang, 2007; Lee & Kim, 1995). Therefore, investigating the causes of windshield yellowing in high-speed trains and providing technical solutions to address these issues is of critical importance.

2. Experiment

2.1 Test materials

Take samples of windshield material measuring 30 × 30 mm from the high-speed train, with test areas designated as A and B, as shown in Figure 2.

2.2 Test method

2.2.1 Corrosion product surface morphology analysis. Cut a 10 × 10 mm sample from the windshield sample. Use a scanning electron microscope (TESCAN MIRA4) to observe and analyze the outer surface of the windshield. Analyze the elemental composition and distribution of the outer surface using the Xplore 30 X-ray spectrometer mounted on the SEM.

Select typical areas of yellowing on the outer surface of the windshield, and use a handheld portable microscope (Anyth) to observe the macro corrosion morphology of the sample. The microscope has a pixel count of 1.8 million and a resolution of 1280×1024 (MJPG).

2.2.2 Effect of UV aging on windshield rubber. Cut a new windshield rubber sample measuring 70 × 150 mm, as shown in Figure 3. Coat the sample surface with deionized water and conduct an ultraviolet aging test in accordance with GB/T 14,522–2008 “Artificial

Figure 1. Yellowing of windshield rubber. **Source(s):** Author’s own work

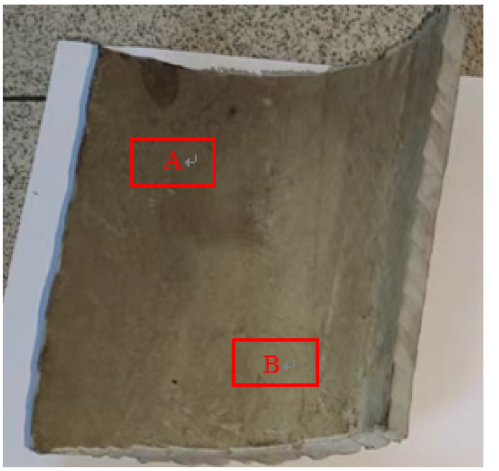

Figure 2. Cutting windshield material. **Source(s):** Author's own work

Figure 3. Newly manufactured windshield rubber test specimen. **Source(s):** Author's own work

Climate Aging Test Methods for Plastics, Coatings, and Rubber Materials Used in Mechanical Products—Fluorescent Ultraviolet Lamp." Take samples once a week and record the gloss and color difference data.

2.2.3 Effect of natural aging on windshield rubber. Coat new windshield rubber test specimens with deionized water and subject to natural aging tests (the specimens are positioned at a 45° angle to the horizon, with the exposed surfaces receiving the maximum amount of solar radiation). Take samples once a week, and record the gloss and color difference data.

2.2.4 Effect of salt spray aging on windshield rubber. Subject new windshield rubber test specimens to salt spray aging tests in accordance with GB/T 10,125–2021 "Artificial Atmosphere Corrosion Tests—Salt Spray Test." Model of salt spray test chamber: LRHS-1080-RY, 5% sodium chloride solution; spray pressure of 98 kPa ± 10 kPa; concentration of collected spray solution of 50 g/L ± 5g/L. Take samples once a week, and record the gloss and color difference data.

2.2.5 Effect of cleaning agents on windshield rubber. Following the method specified in GB/T 1690 "Test Methods for Resistance of Vulcanized Rubber or Thermoplastic Rubber to Liquids," immerse windshield rubber samples in acidic cleaning agent (10% by mass), neutral cleaning agent (10% by mass), alkaline cleaning agent (10% by mass), solvent-based cleaning agent, and distilled water for 5 days. Test the mass difference before and after immersion, calculate the mass change rate and hardness change. The sample dimensions are $5 \times 5 \times 2$ mm.

Perform microscopic photography and SEM testing on the samples.

Infrared spectroscopy (FTIR): use attenuated total reflection to perform infrared testing on the surface of windshield rubber samples before and after immersion in different cleaning agents.

AFM testing: take windshield rubber samples with dimensions of 5×5 mm and a surface roughness not exceeding 5 μm, and test the sample surfaces. Instrument model: Bruker Dimension Icon.

3. Results and discussion

3.1 Composition of yellowing deposits

Collect contaminants adhering to the outer surface of the high-speed train, and apply adhesive tape near the windshield position as shown in Figure 4. After sampling, analyze the main components of the contaminants (comparing the blank adhesive tape before testing with the contaminated adhesive tape after testing), as shown in Table 1 and Figure 5.

Analysis indicates that trace elements such as Mg and Al may precipitate from the aluminum alloy vehicle body; Na, K, and Cl originating from inorganic salts present in rainwater; Ca^{2+} and CO_3^{2-} derive from airborne particulate matter; iron filings generated by rail friction contain Fe, Mn, Cr, Ni, and other trace alloys; and organic oils stem from fuel injection equipment or vehicle-added oil mixtures (Swoger, 2012; Nagai, Ogawa, Nishimoto, & Ohishi, 1999; Awasthi & Agarwal, 2010).

Figure 4. Adhesive tape application. **Source(s):** Author's own work

Table 1. Analysis of the components of contaminants adhering to the exterior surfaces of the EMU

Element	Weight %
C	31.54
O	22.22
F	1.26
Na	1.71
Mg	0.66
Al	0.97
Si	1.60
Zr	2.79
Mo	0.53
Cl	0.34
K	0.22
Ca	0.24
Cr	0.22
Mn	0.35
Fe	34.39
Co	0.53

Source(s): Author's own work

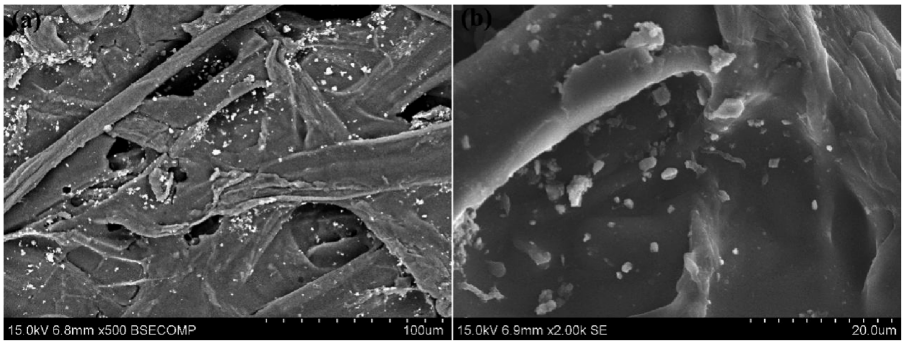

Figure 5. Morphology of contaminants. **Source(s):** Author's own work

3.2 Microstructural morphology of yellowed windshield rubber materials

The corrosion product morphology of the windshield rubber areas A and B on the vehicle body was photographed using a handheld microscope, with two points photographed in each area. It can be observed that the outer surface of the windshield exhibits cracks accompanied by bright white and dark gray corrosion spots, as shown in Figure 6.

Surface morphology observations were conducted on the corrosion products of the outer surface areas A and B of the yellowed windshield rubber, and their compositions were analyzed using EDS and point scanning. The results are shown in Table 2 and Figure 7.

C racks were observed on the surface of the windshield material, with higher proportions of C, O, Si, and Ba elements at the crack sites. This is primarily due to the aged and rough outer surface of the windshield material, which easily accumulates more dust and dirt. The presence of trace amounts of Al, Fe, Mg, and Na may be introduced by metal elements from vehicle operation friction. Additionally, corrosive elements such as S and P were detected on the material surface, which may have a corrosive effect on the windshield material (Docquier, Fisette, & Jeanmart, 2008; Zhu, Yang, Zhang, Feng, & Ma, 2017; Sreenivasan & Keppanan, 2019; Lee, Kim, & Huh, Kim, & Jeong, 2003).

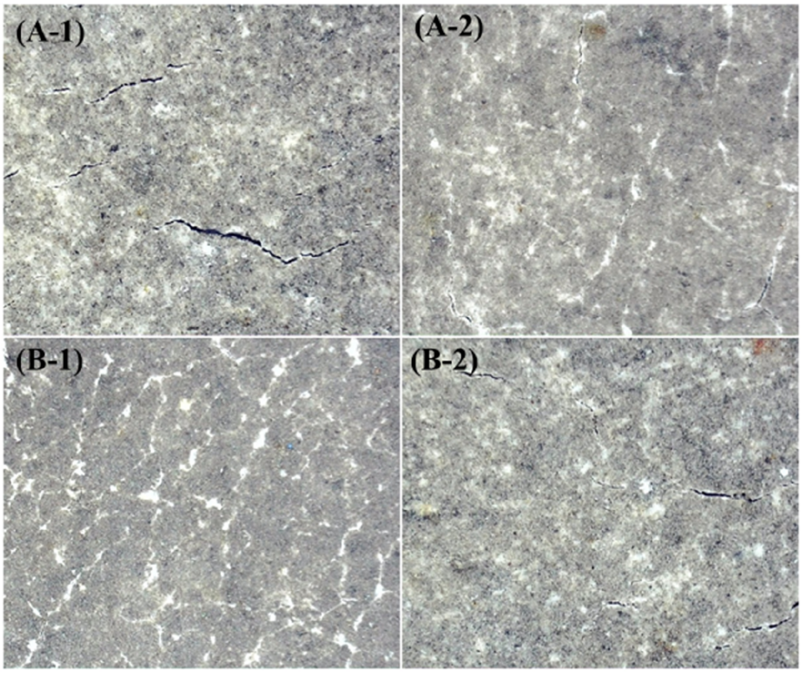

Figure 6. Morphology of corrosion products on windshield rubber. **Source(s):** Author's own work

Table 2. Component analysis of corrosion products on the outer surface of the yellowed windshield rubber

Element	Weight % A	B
C	19.41	17.79
O	44.11	33.66
Al	5.99	3.27
Si	11.28	9.22
S	3.66	5.53
Ba	11.26	24.5
Fe	1.67	3.38
P	0.29	0.24
K	0.51	0.56
Ca	0.74	1.01
Mg	0.59	0.46
Na	0.49	0.37

Source(s): Author's own work

3.3 UV aging test analysis

Windshield rubber test samples coated with clean water showed that, as UV aging time increased, color difference remained stable at 10–12 after 288 h, while gloss continued to decrease to 5–15. UV radiation and thermal oxidation synergistically accelerate the consumption of antioxidants (such as phenols and amines) (Mazzola & Berg, 2014). Once antioxidants migrate to the surface of the windshield rubber, they will become ineffective due to oxidation and fail to capture free radicals, leading to continued oxidative reactions

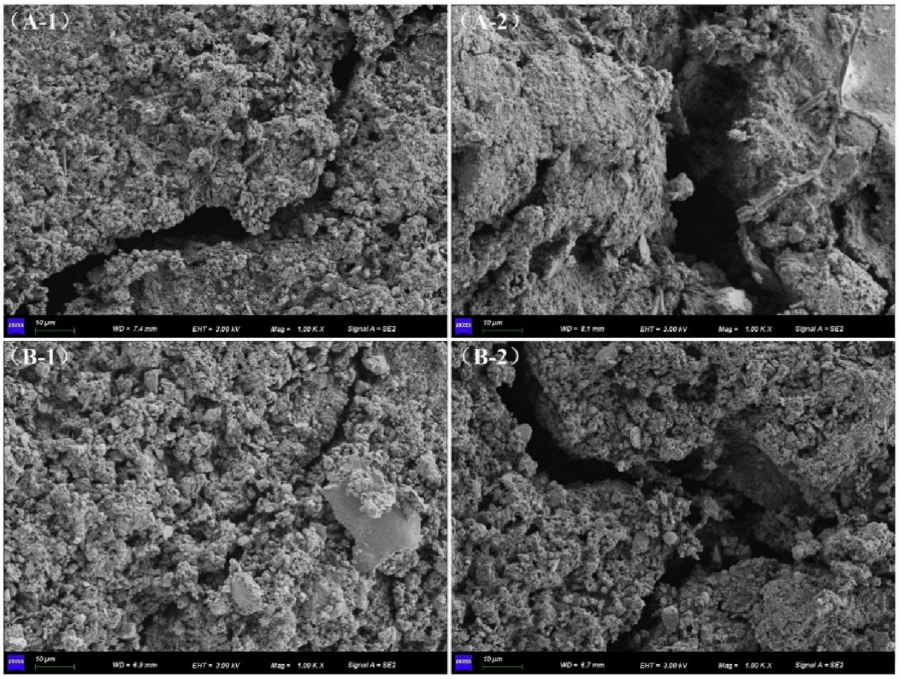

Figure 7. Electron microscope image of the appearance of yellowed windshield rubber. **Source(s):** Author's own work

within the material and resulting in color difference and gloss reduction. Therefore, UV irradiation is the primary factor causing color change in windshield rubber, as shown in Figures 8 and 9.

The changes in gloss and color difference of windshield rubber are primarily caused by material aging and the complex interaction with the environment: windshield rubber materials are primarily EPDM rubber or silicone rubber. Under long-term UV irradiation (cumulative UVB dose≥120 kJ/m^2) and temperature cycling (−40°C to +70°C), the polymer chains undergo photo-oxidative degradation, leading to the migration of plasticizers and the failure of antioxidants, resulting in surface yellowing. The electron microscopy results show that white patches appear on the surface of the windshield rubber after 288 hours, and the aging and whitening phenomenon intensify with time, as shown in Figure 10.

UV aging is mainly caused by polymer photochemical reactions triggered by ultraviolet radiation, leading to structural damage and performance degradation of rubber materials. High energy photons in ultraviolet radiation (especially in the UV-A and UV-B bands with wavelengths of 300–400 nm) are absorbed by rubber molecules, directly damaging weak areas in the molecular chain (such as unsaturated double bonds), and generating highly active free radicals. These free radicals react rapidly with oxygen (O_2) to form peroxide free radicals ($RO_2\cdot$), which then attack other molecular chains, trigger chain degradation, break molecular chains, and cause rubber elasticity loss, softening, or pulverization.

3.4 Natural aging test analysis

Windshield rubber samples coated with water exhibited minimal changes in color difference and gloss after 432 h of natural aging. This was due to the gradual stabilization of the surface oxidation layer, which reduced the reaction rate of active groups, causing color difference and

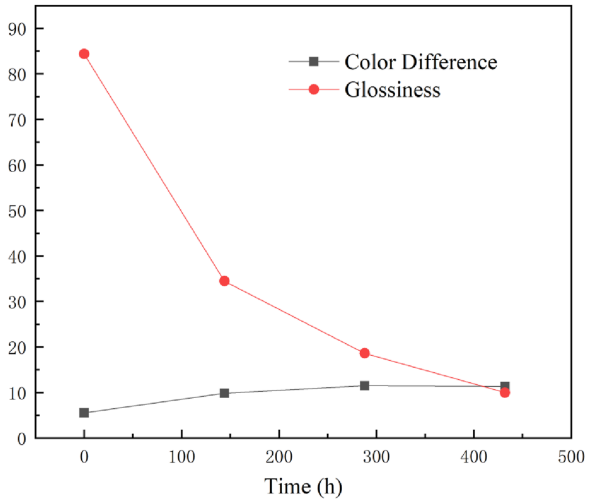

Figure 8. Gloss and color difference of windshield rubber after UV aging. **Source(s):** Author's own work

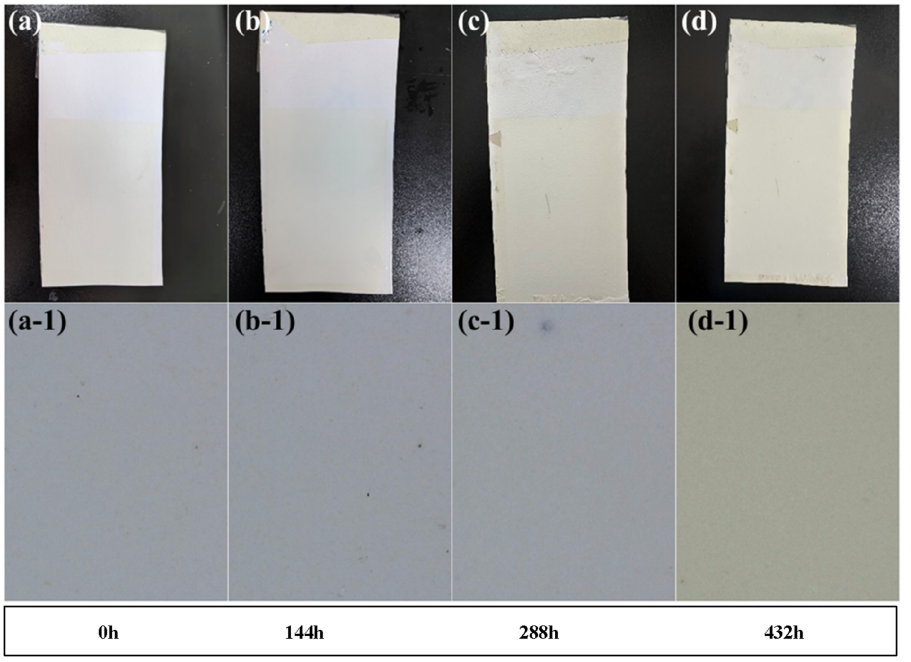

Figure 9. UV-aged windshield rubber samples and microscopic images. **Source(s):** Author's own work

gloss changes to plateau (Facchinetti, Mazzola, Alfi, & Bruni, 2010; Jeong, Song, Huh, Kim, & Kim, 2006). Natural aging was a slow and gradual process, as shown in Figures 11 and 12.

Natural aging is caused by the synergistic effects of environmental factors (ultraviolet radiation, oxygen, and temperature fluctuations) that disrupt the molecular structure of

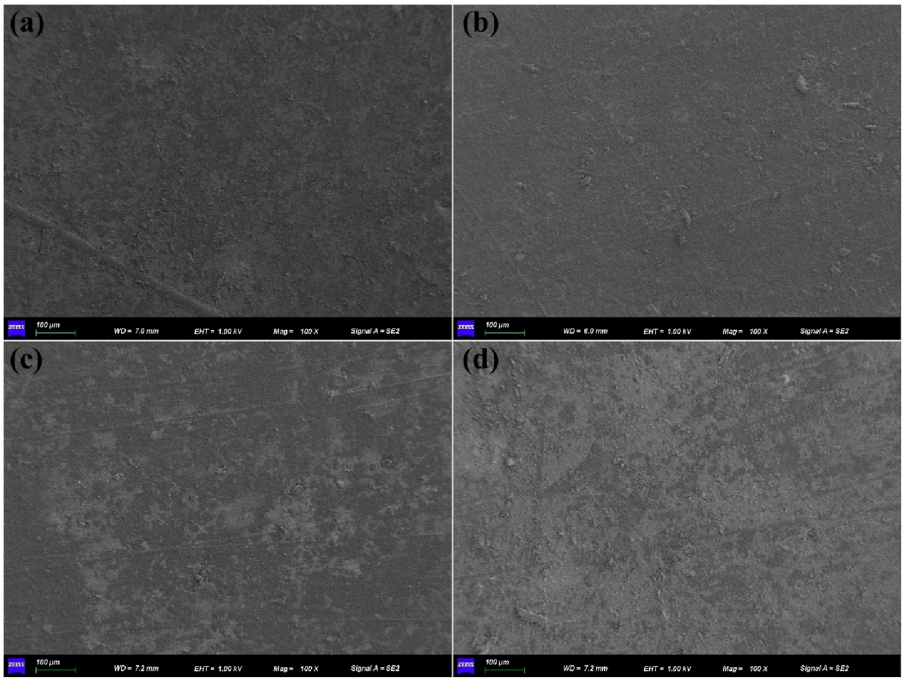

Figure 10. Electron microscopy image of windshield rubber after UV aging. **Source(s):** Author's own work

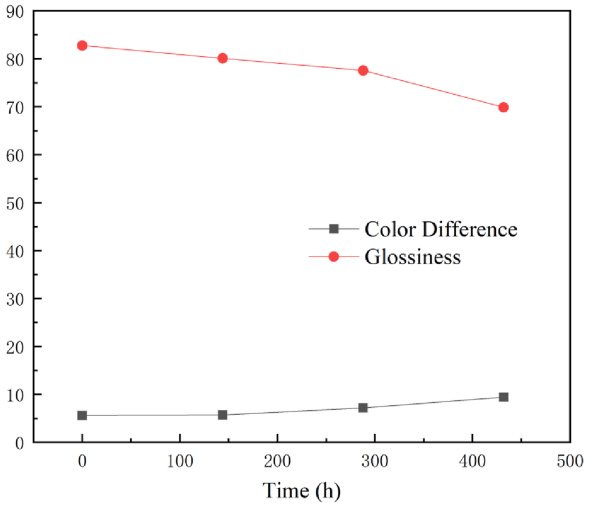

Figure 11. Gloss and color difference of windshield rubber after natural aging. **Source(s):** Author's own work

rubber. Oxidation reactions dominate: oxygen penetration causes the oxidation and breakage of rubber molecular chains, generating oxygen-containing groups such as carbonyl and carboxyl groups, resulting in a significant decrease in material elasticity. UV photolysis: UV radiation (280–400 nm) provides energy to break C-C bonds (347 kJ/mol)

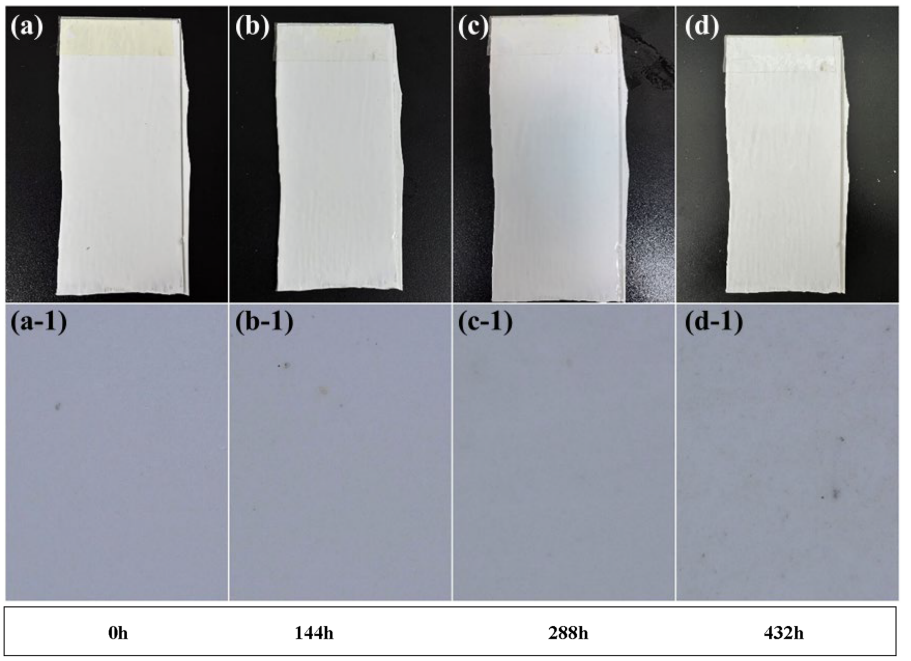

Figure 12. Test specimens and micrographs of windshield rubber after natural aging. **Source(s):** Author's own work

and C-H bonds (413 kJ/mol), generating free radicals and triggering chain degradation, accelerating surface brittleness. High temperatures accelerate the diffusion rate of oxygen molecules, speeding up the oxidation reaction process. Simultaneously, temperature fluctuations cause stress accumulation within the rubber, leading to the propagation of microcracks. The effect of natural aging on rubber is a gradual, slow degradation process driven by multiple factors.

There are differences in the aging phenomenon of rubber samples after UV aging and natural aging. UV aging is a rapid and irreversible process of molecular chain breakage caused by ultraviolet radiation in the short term. Cracks, roughness, powdering, whitening, or discoloration appear on the surface of UV aging (often seen in exposed areas). The physical performance is manifested as the direct breakage of molecular chains leading to rapid loss of elasticity and significant decrease in mechanical properties. UV aging triggers a chain reaction to accelerate oxidation, with cracks perpendicular to the stress direction. However, natural aging is dominated by thermal oxidative reactions, which slowly accumulate damage over time and temperature, and the process is relatively uniform. Natural aging causes the surface to become uniformly thinner, harden or soften as a whole, and slowly form fine lines. The physical properties manifest as gradual molecular structure breakdown (cross-linking/degradation) and gradual decrease in elasticity.

3.5 Salt spray aging test analysis

Windshield rubber specimens coated with water showed minimal changes in color difference and light color after 432 hours of salt spray aging, indicating that the effect of salt spray aging on the rubber specimens was negligible, as shown in Figures 13 and 14.

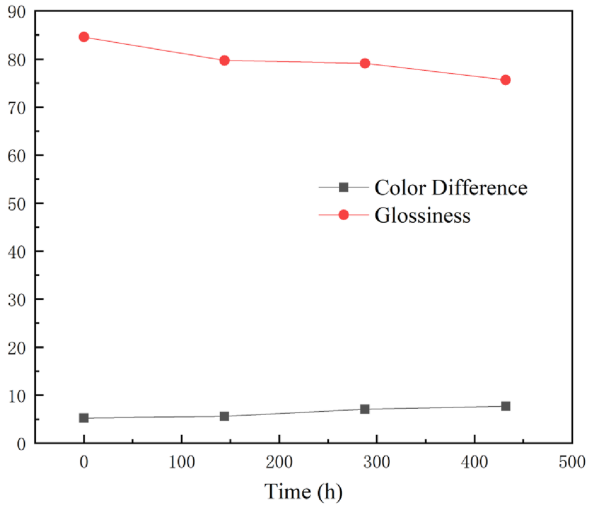

Figure 13. Gloss and color difference of windshield rubber after salt spray aging. **Source(s):** Author's own work

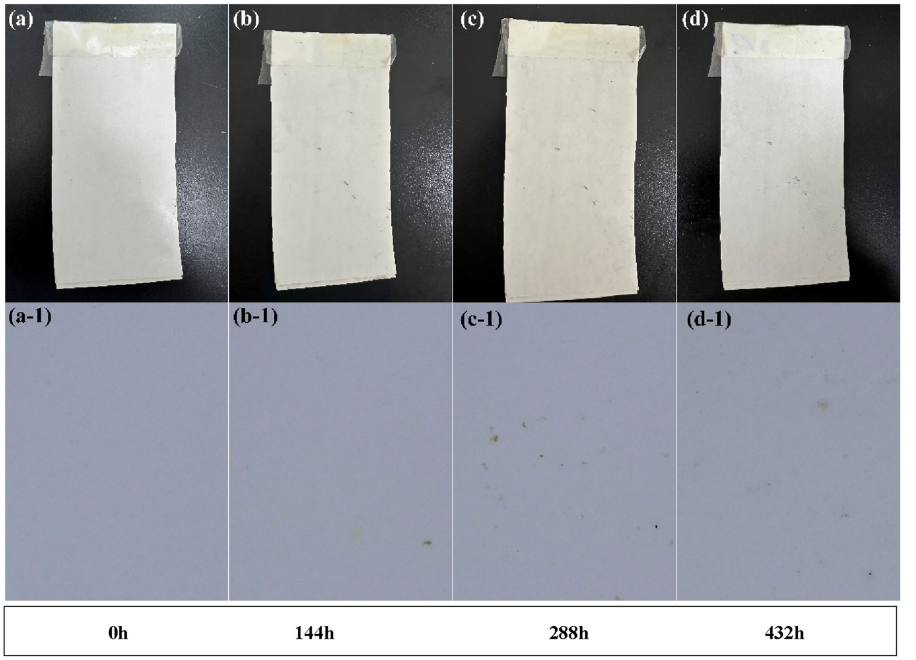

Figure 14. Windshield rubber samples and micrographs after salt spray aging. **Source(s):** Author's own work

3.6 Cleaning agent test analysis

3.6.1 Immersion corrosion test. Following the method specified in GB/T 1690 "Test Methods for Resistance of Vulcanized Rubber or Thermoplastic Rubber to Liquids," windshield rubber

samples were immersed in acidic cleaning agent (10% by mass), neutral cleaning agent (10% by mass), alkaline cleaning agent (10% by mass), solvent-based cleaning agent, and distilled water for 5 days. The mass difference before and after immersion was measured, and the mass change rate and hardness change were calculated, as shown in Table 3 and Figure 15. It can be observed that the mass change rate of the windshield rubber immersed in different solutions is as follows: acidic cleaning agent > alkaline cleaning agent > solvent-based cleaning agent > distilled water > neutral cleaning agent; the hardness change is as follows: solvent-based cleaning agent > acidic cleaning agent > alkaline cleaning agent > distilled water > neutral cleaning agent.

Rubber materials contain active groups such as benzene rings, allyl groups, -OH, and C-= -C in their molecular structure. In acidic, alkaline, or solvent environments, these groups undergo complex chemical reactions, leading to significant changes in physical and chemical properties. This not only involves the breakage and recombination of molecular chains, but also results in the deterioration of macroscopic properties, with solvents physically penetrating and disrupting the structure. In acidic environments, H^+ ions attack double bonds, triggering oxidative cleavage and generating free radical intermediates, which further accelerate auto-oxidation chain reactions. This results in the rubber losing its elasticity and the surface developing cracks. In alkaline environments, the rubber is easily attacked by hydroxide ions (OH^-) through nucleophilic reactions, causing ring opening or substitution reactions in the benzene ring, disrupting the rigid molecular chain structure, leading to softening and swelling of the rubber material. Therefore, the quality change rate is highest for acidic and alkaline

Table 3. Corrosion quality and hardness changes of windshield rubber

Material	Acidic cleaning agent (10% by mass)	Neutral cleaning agent (10% by mass)	Alkaline cleaning agent (10% by mass)	Solvent-based cleaning agent	Distilled water
Mass change rate	2.05	0.81	1.53	1.39	1.28
Hardness change	0.58	0.12	0.38	0.91	0.31

Source(s): Author's own work

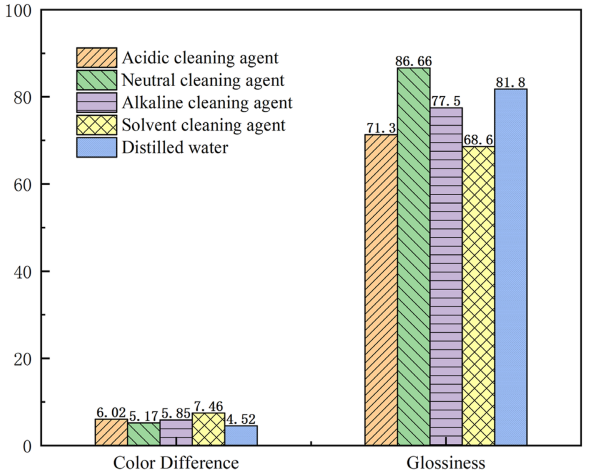

Figure 15. Gloss and color difference of windshield rubber after immersion in different cleaning agents for 5 days. **Source(s):** Author's own work

cleaning agents. Prolonged contact with solvents causes non-polar solvents to penetrate the rubber network, weakening intermolecular forces and causing surface swelling, resulting in the greatest hardness change. However, in this test, the quality change rate and hardness change values of the windshield rubber are similar to those of distilled water and within reasonable ranges. It is inferred that the main components of the cleaning agents are non-ionic surfactants, additives, and corrosion inhibitors, with extremely low additions of acidic, alkaline, or solvent substances. Therefore, after dilution, the effective content is extremely low, and it can be considered that diluted acidic, alkaline, and solvent cleaning agents have a minimal impact on rubber.

3.6.2 SEM morphology after immersion. SEM surface morphology observations were conducted on the windshield rubber. The observations revealed a smooth and intact surface with no obvious signs of corrosion. Elemental analysis indicated that the windshield rubber was primarily composed of three elements: C, O, and Si, with C being the most abundant. Additionally, trace amounts of metallic elements such as Zn, Mg, and Al were detected, while trace amounts of S and N might have been introduced from the atmospheric environment. The results were shown in Figure 16 and Table 4.

3.6.3 Infrared spectroscopy testing (FTIR). Infrared testing was conducted on the sample surfaces before and after immersion in the cleaning agent using attenuated total reflection. The results are shown in Figure 17. From the infrared spectra, it can be seen that 750 cm^{-1} may be the absorption peak of the (CH_2) vibration, 1078 cm^{-1} may be the absorption peak of the C-O vibration, and 1458 cm^{-1} may be the absorption peak of Si (CH_3) 2 vibration peak absorption peak, 1609 cm^{-1} may be the C=C vibration peak absorption peak, indicating that the compound contains CH (3) and CH (2), 1745 cm^{-1} may be the conjugated C=O absorption peak, and 2913 cm^{-1} and 2849 cm^{-1} may be absorption peaks of saturated hydrocarbon C-H stretching vibrations. The peaks at 2913 cm^{-1}, 2849 cm^{-1}, 1745 cm^{-1}, 1609 cm^{-1}, 1458 cm^{-1}, 1078 cm^{-1}, and 750 cm^{-1}, indicating that the structural integrity of the windshield rubber samples remain unchanged after immersion in the cleaning agent. This further confirms that the diluted cleaning agent has negligible effects on the windshield rubber.

3.6.4 Atomic force microscopy (AFM). AFM (German Bruker Dimension Icon) was used to observe the surface morphology of the samples before and after immersion in the cleaning agent. The results are shown in Figure 18. After immersion in the cleaning agent, the surface morphology of the samples undergoes minor changes. The surface roughness of the five windshield rubber samples after immersion is as generally between −250 nm and −200 nm, further confirming that the diluted cleaning agent has virtually no effect on the windshield rubber.

4. Countermeasures

4.1 Specialized cleaning agents

There are two kinds of specialized cleaning agents, including metal oxide stains: reddish-brown rust deposits formed by the oxidation of metal particles from rail friction or industrial dust; organic stains: accumulation of oil residues, atmospheric pollutants, and other micro-particles over time.

The above-mentioned yellow spot stains are washable. The specialized cleaning agents use a special raw material compounding process and contain small molecule chelating agents, which can chelate with divalent cationic metals (calcium, magnesium, iron, etc.) contained on the surface of the yellow spot. Although the chelated complexes adsorb onto the paint surface, their water solubility is enhanced under the action of cationic surfactants, and they no longer continue to grow and undergo lattice distortion, making it easy for scale to disperse and remove. The yellow spot removal rate is over 85%, which can effectively solve the problem of yellow spots on the outer surface of high-speed trains, as shown in Figure 19.

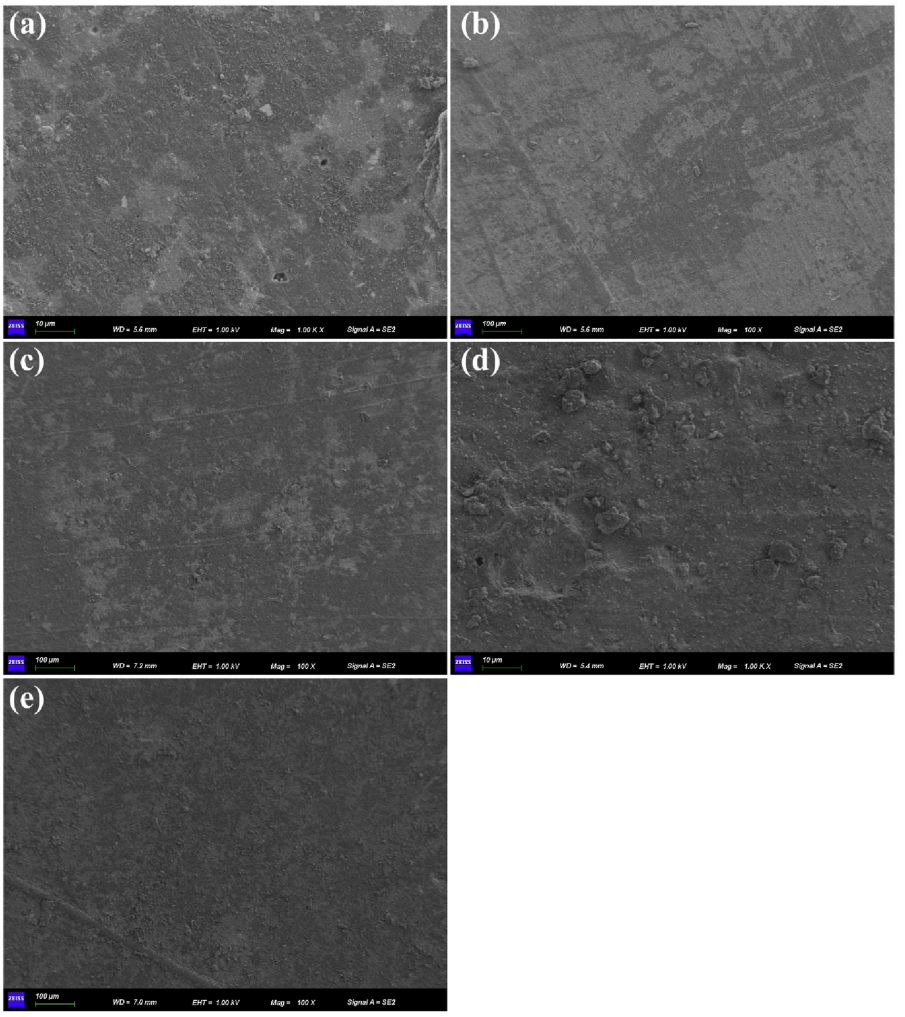

Figure 16. SEM images of the windshield rubber surface after immersion (a) immersion in acidic cleaning agent (b) immersion in neutral cleaning agent (c) immersion in alkaline cleaning agent (d) immersion in solvent cleaning agent (e) immersion in distilled water. **Source(s):** Author's own work

4.2 Yellow stain repair agent

Aging yellowing: an irreversible chemical degradation phenomenon that occurs in polymer coatings under long-term exposure to ultraviolet radiation. The mechanism is that ultraviolet radiation (295–360 nm band) triggers the breakage of resin molecular chains, especially the aromatic structures in polyurethane or acrylic polyurethane topcoats. After absorbing ultraviolet photons, quinone chromophores are generated through photooxidation reactions. This process follows a free radical chain reaction: ultraviolet radiation first breaks chemical bonds to produce alkyl radicals, which then react with oxygen to form hydroperoxides. Finally, through beta cleavage, carbonyl compounds (such as aldehydes and ketones) are generated, causing the material to turn yellow and cannot be removed by physical cleaning. This type of

Table 4. Elemental composition of the outer surface of windshield rubber specimens after immersion in different solutions

Element	Weight percentage (wt%) Soaked in acidic cleaning agent	Neutral cleaning agent immersion	Alkaline cleaning agent immersion	Solvent cleaner immersion	Distilled water immersion
C	72.17	68.97	69.28	62.44	72.32
O	22.76	27.69	25.42	25.76	23.48
Si	0.70	0.62	0.52	1.17	0.75
Zn	2.81	1.93	3.73	2.22	1.81
F	1.24	0.20	/	2.49	1.12
Al	0.20	0.13	0.51	0.21	0.25
S	0.13	0.1	/	0.18	0.13
N	/	/	0.61	5.29	0.13
Total	100	100	100	100	100

Source(s): Author's own work

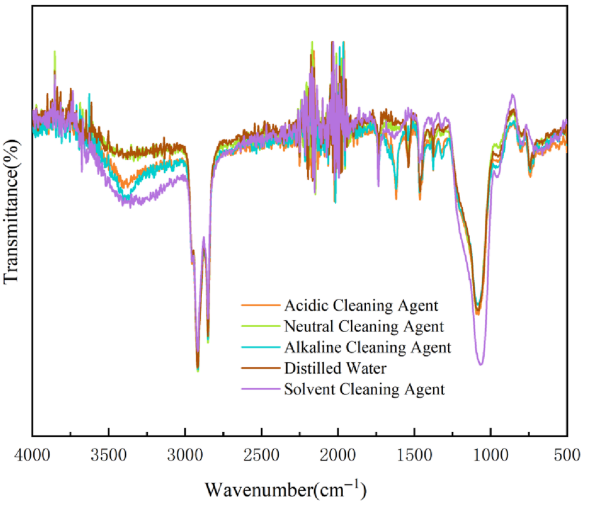

Figure 17. Infrared spectrum of windshield rubber after immersion in cleaning agent. **Source(s):** Author's own work

yellowing can be repaired by spraying with repair agents, adding ultraviolet absorbers (such as benzotriazoles), or using aliphatic polyurethane to delay yellowing. After polishing, a more weather resistant nano modified repair agent can be reapplied, as shown in Figure 20.

5. Conclusions

(1) Under UV aging conditions, antioxidants in windshield rubber migrate to the surface, where they become ineffective due to oxidation and fail to capture free radicals, leading to continued oxidative reactions within the material and resulting in rapid aging and yellowing of the rubber.

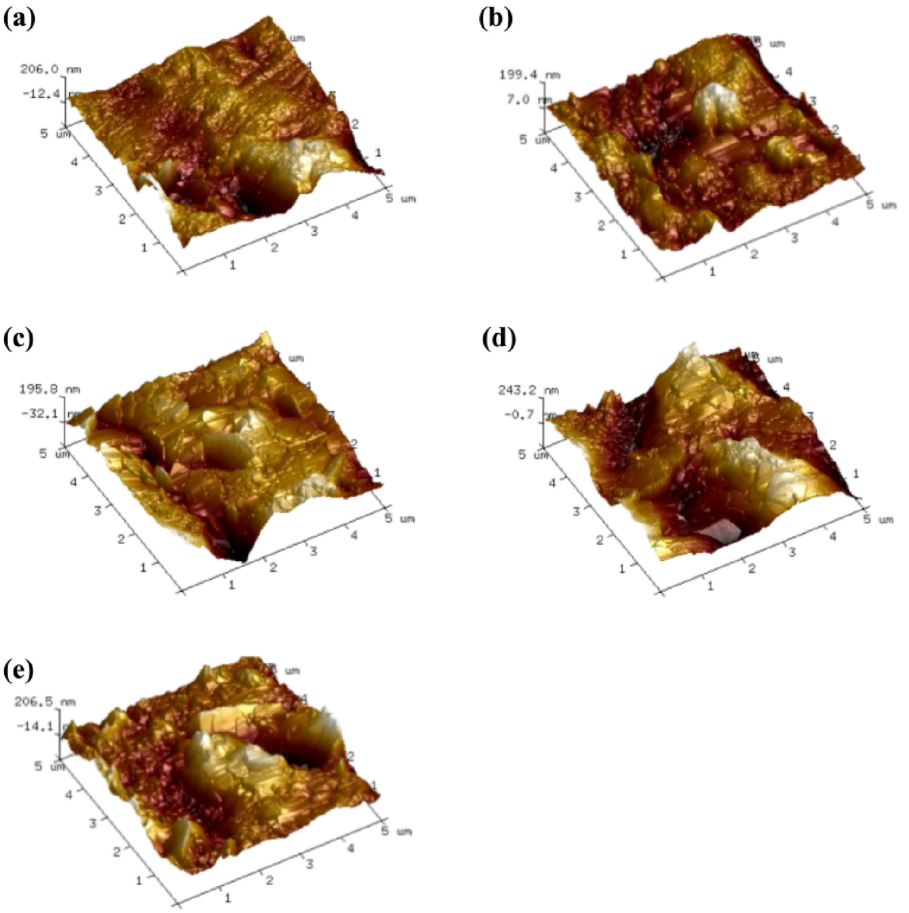

Figure 18. Atomic force microscopy images of windshield rubber after UV aging: (a) immersion in acidic cleaning agent, (b) immersion in neutral cleaning agent, (c) immersion in alkaline cleaning agent, (d) immersion in solvent cleaning agent, (e) immersion in distilled water. **Source(s):** Author's own work

Figure 19. Windshield cleaning. **Source(s):** Author's own work

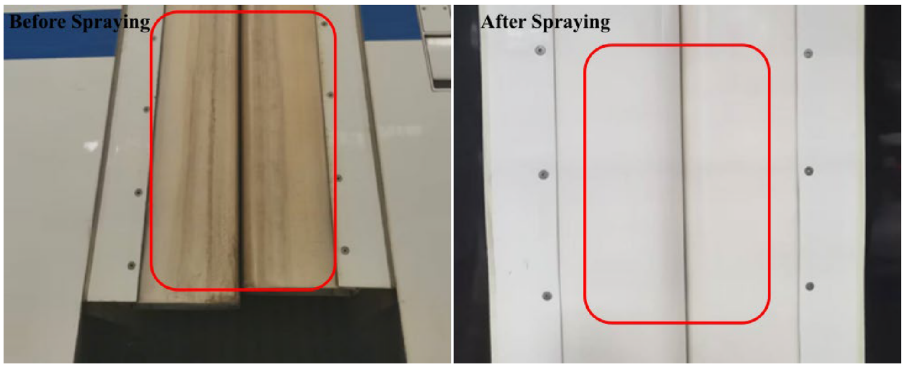

Figure 20. Windshield repair. **Source(s):** Author's own work

(2) The effect of natural aging on windshield rubber is a gradual, slow deterioration process driven by multiple factors. However, UV aging has a significantly greater impact on windshield rubber than natural aging.

(3) Diluted cleaning agents, whether acidic, neutral, alkaline, or solvent-based, have minimal impact on windshield rubber.

(4) Cleaning cycles should be determined based on vehicle models and operational environments, with recommendations for two types of cleaning: routine cleaning and deep cleaning. Routine cleaning involves quick cleaning and should be conducted in conjunction with daily maintenance. Deep cleaning targets stubborn stains and should be performed during vehicle inspections or specialized repairs.

References:

Awasthi, S., & Agarwal, D. (2010). Preparation and characterisation of polyurethane coatings based on polyester polyol. *Pigment and Resin Technology*, *39*(4), 208–213. doi: 10.1108/03699421011055518.

Celina, M. C. (2013). Review of polymer oxidation and its relationship with materials performance and lifetime prediction. *Polymer Degradation and Stability*, *98*(12), 2419–2429. doi: 10.1016/j.polymdegradstab.2013.06.024.

Docquier, N., Fisette, P., & Jeanmart, H. (2008). Model-based evaluation of railway pneumatic suspensions. *Vehicle System Dynamics*, *46*(Supplement 1), 481–493. doi: 10.1080/00423110801993110.

Facchinetti, A., Mazzola, L., Alfi, S., & Bruni, S. (2010). Mathematical modelling of the secondary airspring suspension in railway vehicles and its effect on safety and ride comfort. *Vehicle System Dynamics*, *48*(Supplement 1), 429–449. doi: 10.1080/00423114.2010.486036.

Ge, H. J. (2010). Research on the scheme of installing friction plate and end-spine on CRTS – slab ballastless track on bridge of Zhengzhou-Wuhan passenger dedicated line. *Journal of Railway Engineering Society*, *2*(19), 3–10.

Huang, J., Wang, J., Qiu, Y., & Wu, D. (2016). Mechanical properties of thermoplastic polyester elastomer controlled by blending with poly (butylene terephthalate). *Polymer Testing*, *55*, 152–159. doi: 10.1016/j.polymertesting.2016.08.020.

Jeong, S. H., Song, J. H., Huh, H., Kim, J. W., & Kim, J. Y. (2006). 3-D finite element modeling of fiber reinforced rubber composites using a rubber element. *Transactions of the Korean Society of Mechanical Engineers-A*, *30*(12), 1518–1525. doi: 10.3795/ksme-a.2006.30.12.1518.

Jiang, H., Zheng, Z., Song, W., Li, Z., & Wang, X. (2007). Alkoxysilane functionalized polyurethane/polysiloxane copolymers: Synthesis and the effect of end-capping agent. *Polymer Bulletin*, *59*(1), 53–63. doi: 10.1007/s00289-007-0748-y.

Kim, G. H., Lee, Y. S., & Yang, H. L. (2016). A new design concept of metal O-ring seal for long-term performance. *Vacuum*, *123*, 54–61. doi: 10.1016/j.vacuum.2015.10.014.

Kim, J., Kim, Y., & Cho, Y. (2025). Estimation of synthetic rubber lifespan based on ozone accelerated aging tests. *Polymers*, *17*(6), 819. doi: 10.3390/polym17060819.

Lee, J. S., & Kim, B. K. (1995). Poly (urethane) cationomers from poly (propylene) glycol and isophorone diisocyanate: Emulsion characteristics and tensile properties of cast films. *Progress in Organic Coatings*, *25*(4), 311–318. doi: 10.1016/0300-9440(95)00551-o.

Lee, H. W., Kim, S. H., Huh, H., Kim, J. Y., & Jeong, S. G. (2003). Finite element analysis of diaphragm-type air springs with fiber-reinforced rubber composites. *Journal of Composite Materials*, *37*(14), 1261–1273. doi: 10.1177/0021998303037014003.

Liu, X. G., Qi, S., Wan, D. T., & Zheng, D. Z. (2022). Study on dynamic response of high speed train window glass under tunnel aerodynamic effects. *Railway Sciences*, *2*(2), 211–224. doi: 10.1108/rs-03-2023-0013.

Mazzola, L., & Berg, M. (2014). Secondary suspension of railway vehicles-air spring modelling: Performance and critical issues. *Proceedings of the Institution of Mechanical Engineers, Part F: Journal of Rail and Rapid Transit*, *228*(3), 225–241. doi: 10.1177/0954409712470641.

Nagai, Y., Ogawa, T., Nishimoto, Y., & Ohishi, F. (1999). Analysis of weathering of a thermoplastic polyester elastomer II. Factors affecting weathering of a polyether–polyester elastomer. *Polymer Degradation and Stability*, *65*(2), 217–224. doi: 10.1016/s0141-3910(99)00007-5.

Sreenivasan, G. P., & Keppanan, M. M. (2019). Analytical approach for the design of convoluted air suspension and experimental validation. *Acta Mechanica Sinica*, *35*(5), 1093–1103. doi: 10.1007/s10409-019-00880-z.

Swoger, B. (2012). Frustration of the day: Unclear article numbers. *Progress in Natural Science*, *22*(1), 71–78.

Tang, M. Z., Xiong, X. H., Li, X. B., Chen, G., Zhang, J., Zhong, M., & Sun, B. (2023). Dynamic response of outer windshield structure in different schemes under aerodynamic load. *Applied Sciences*, *13*(6), 3879. doi: 10.3390/app13063879.

Wu, D., Wang, S., & Wang, X. (2017). A novel stress distribution analytical model of O-ring seals under different properties of materials. *Journal of Mechanical Science and Technology*, *31*(1), 289–296. doi: 10.1007/s12206-016-1231-1.

Xu, X., Song, Y., Zheng, Q., & Hu, G. (2007). Influence of Incorporating $CaCO_3$ into room temperature vulcanized silicone sealant on its mechanical and dynamic rheological properties. *Journal of Applied Polymer Science*, *103*(3), 2027–2035. doi: 10.1002/app.25324.

Yang, M., & Jiang, H. W. (2011). Influences of NCO-based polyorganosiloxane primer on bonding properties of polyurethane sealant. *China Adhesives*, *6*(16), 8–13.

Yu, Q. P., Sun, J. J., Ma, C. B., & Zhang, Y. Y. (2019). A percolation method of leakage calculation and prediction within the mechanical seal interface. *Journal of Tribology*, *141*(12), 122203. doi: 10.1115/1.4044671.

Zhang, W. H., Zeng, Y. C., Song, D. L., & Wang, Z. W. (2024). Theory and practice for assessing structural integrity and dynamical integrity of high-speed trains. *Railway Sciences*, *3*(2), 113–127. doi: 10.1108/rs-01-2024-0002.

Zhu, H., Yang, J., Zhang, Y., Feng, X., & Ma, Z. (2017). Nonlinear dynamic model of air spring with a damper for vehicle ride comfort. *Nonlinear Dynamics*, *89*(2), 1545–1568. doi: 10.1007/s11071-017-3535-9.

Corresponding author
Wei Du can be contacted at: railwaydu@163.com